Supplemental Figure 1

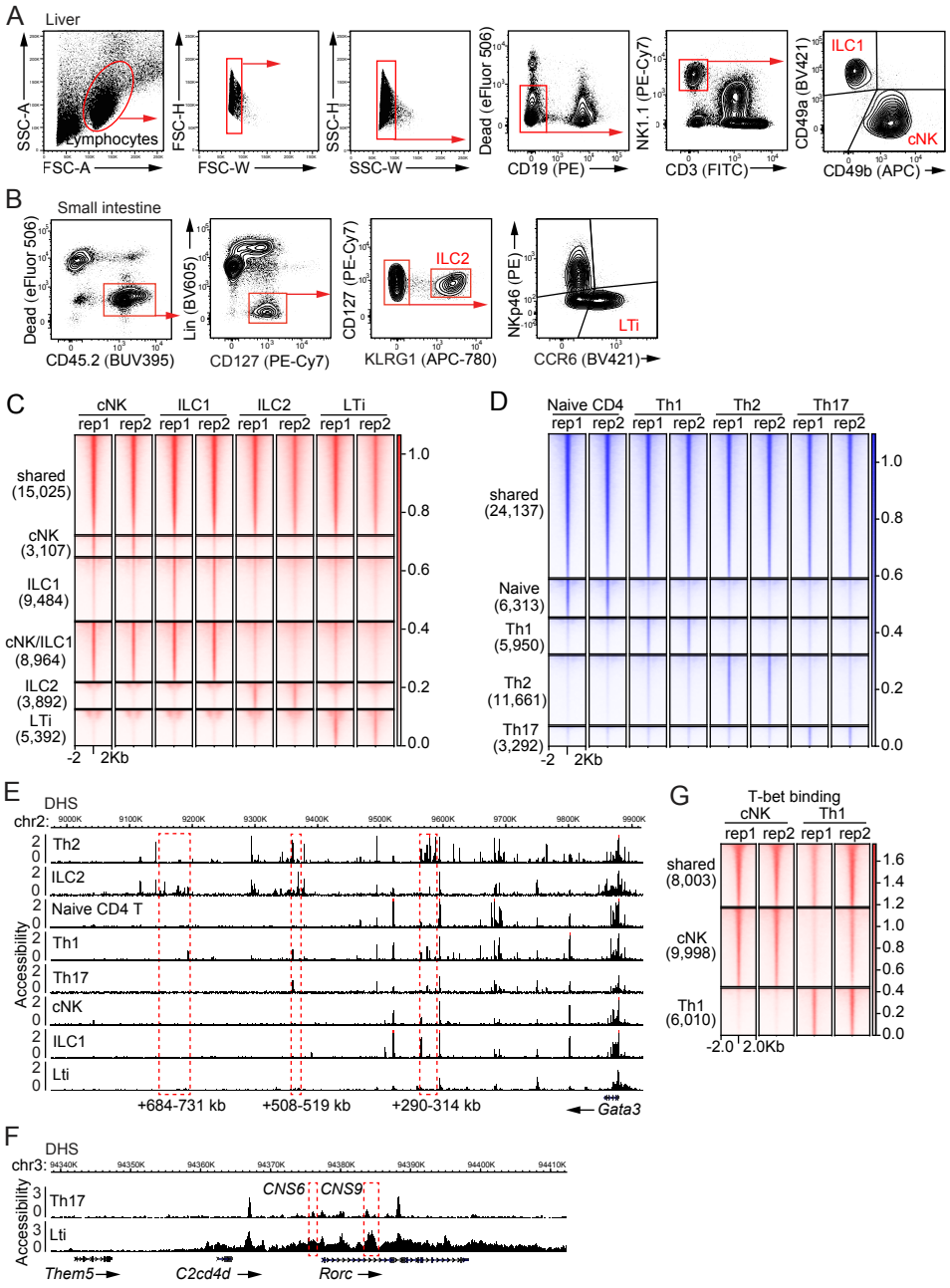

Supplementary Figure 1. Differential chromatin accessibilities in CD4 T cell and ILC subsets, related to Figure 1

(A) The hepatic cNK cells were gated as $CD3^{-}CD19^{-}NK1.1^{+}CD49a^{-}CD49b^{+}$, and the hepatic ILC1s were gated as $CD3^{-}CD19^{-}NK1.1^{+}CD49a^{+}CD49b^{-}$.

(B) The ILC2s were gated as $Lin^{-}CD127^{+}KLRG1^{+}$, and the LTi cells were gated as $Lin^{-}CD127^{+}KLRG1^{-}CCR6^{+}NKp46^{-}$ from the small intestine.

(C) cNK-, ILC1-, cNK/ILC1-, ILC2- and LTi-specific DHSs as well as DHSs shared by all these cell types were analyzed in the innate lymphocyte counterpart.

(D) Naïve CD4 T cell-, Th1-, Th2- and Th17-specific DHSs as well as DHSs shared by all these cell types were analyzed in CD4 T cell counterpart.

(E) Chromatin accessibility at the *Gata3* locus in CD4 T cell and ILC subsets was viewed by Wash U genome browser.

(F) Chromatin accessibility at the *Rorc* locus in Th17 and LTi cells was viewed by Wash U genome browser. The truncated transcript of *Rorc*, which encodes RORγt, was shown.

(G) T-bet binding sites in Th1 and cNK cells were analyzed.

Supplemental Figure 2

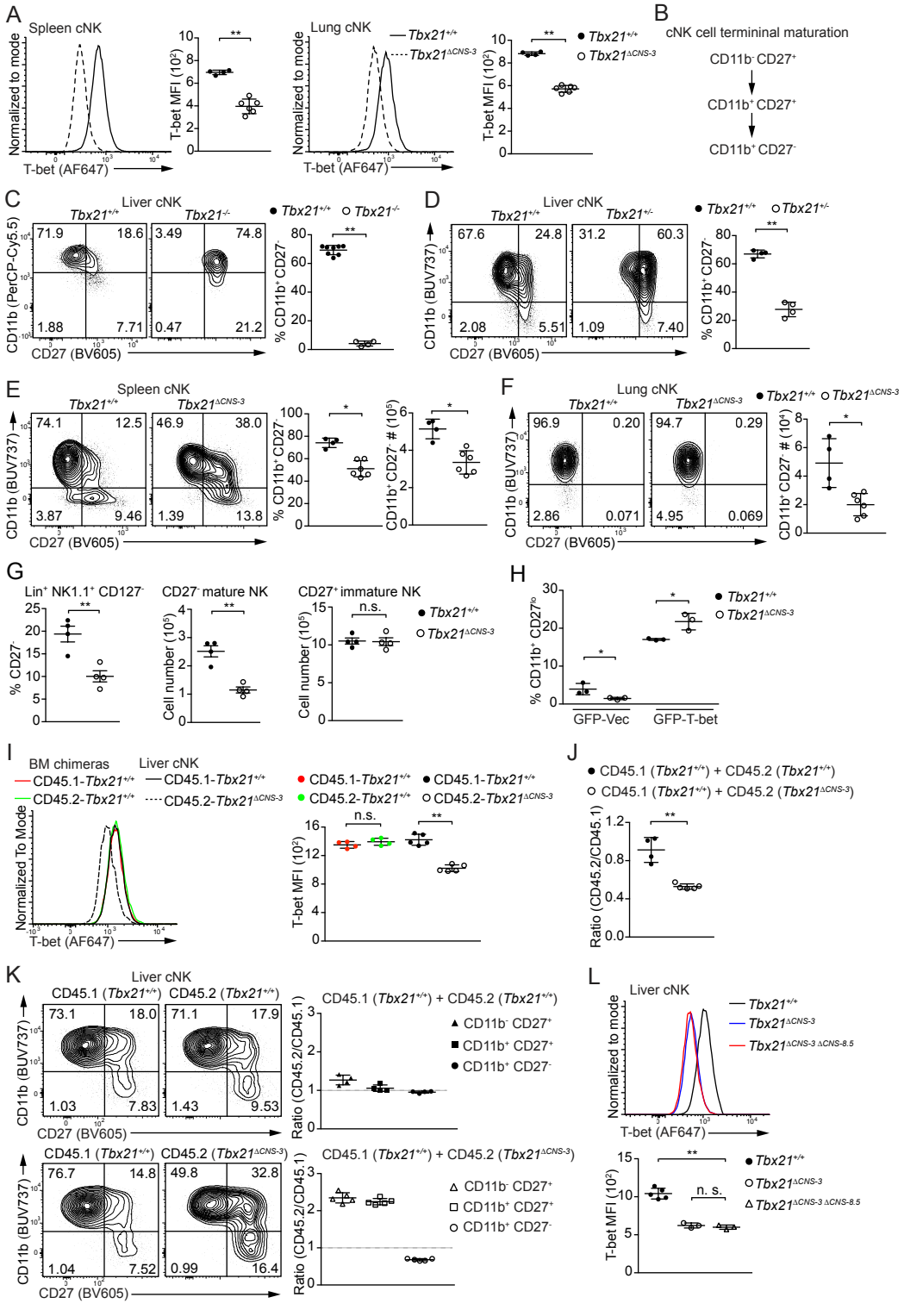

Supplementary Figure 2. A critical role of *Tbx21-CNS-3* for T-bet induction in cNK cells, related to Figure 2

(A) T-bet protein amounts in splenic and pulmonic cNK cells from *Tbx21*$^{+/+}$ (n=4) and *Tbx21*$^{\triangle CNS-3}$ (n=6) mice were measured, and T-bet MFI was calculated. Mean ± SD.

(B) Progression of cNK cell maturation using cell surface proteins CD11b and CD27.

(C) Maturation of hepatic cNK cells from *Tbx21*$^{+/+}$ (n=8) and *Tbx21*$^{-/-}$ (n=4) mice was assessed. The percentage of CD11b^{+}CD27^{-} mature cNK cells was calculated. Mean ± SD.

(D) Maturation of hepatic cNK cells from *Tbx21*$^{+/+}$ (n=4) and *Tbx21*$^{+/-}$ (n=4) mice was assessed. The percentage of CD11b^{+}CD27^{-} mature cNK cells was calculated. Mean ± SD.

(E and F) Maturation of splenic cNK cells (E) and pulmonic cNK cells (F) from *Tbx21*$^{+/+}$ (n=4) and *Tbx21*$^{\triangle CNS-3}$ (n=6) mice was assessed. The percentage and the cell number of CD11b^{+}CD27^{-} mature cNK cells were calculated. Mean ± SD.

(G) BM cells were stained with a lineage cocktail (CD11b, CD3, CD4, CD8, B220, TER119 and Ly6G/6C) together with antibodies to several surface markers for identifying NK cells. The percentage and total cell number of mature (CD27^{-}) and immature (CD27^{+}) NK cells within the NK cell (Lin^{+}NK1.1^{+}CD127^{-}) population from *Tbx21*$^{+/+}$ (n=4) and *Tbx21*$^{\triangle CNS-3}$ (n=4) BM were calculated.

(H) LMPPs (Lin^{-}CD117^{+}Sca1^{+}Flt3^{+}CD127^{-}) from the bone marrow of *Tbx21*$^{+/+}$ (n=3) and *Tbx21*$^{\triangle CNS-3}$ (n=3) mice were cultured 2.5 days before retroviral infection with GFP-T-bet or GFP-Vector control. On day 6, infected cells were further co-cultured with OP9 cell line for additional 8 days. The expression of CD11b and CD27 was assessed on CD19^{-}NK1.1^{+}GFP^{+} populations.

(I-K) CD45.1 *Tbx21*$^{+/+}$ BM cells were co-transferred with either CD45.2 *Tbx21*$^{+/+}$ BM cells or CD45.2 *Tbx21*$^{\triangle CNS-3}$ BM cells at 1:1 ratio into sub-lethally irradiated *Rag2*$^{-/-}$*γc*$^{-/-}$ recipient mice to create CD45.1 *Tbx21*$^{+/+}$/CD45.2 *Tbx21*$^{+/+}$ (n=4) and CD45.1 *Tbx21*$^{+/+}$/CD45.2 *Tbx21*$^{\triangle CNS-3}$ (n=5) mixed chimeras. T-bet protein amounts were measured, and T-bet MFI was calculated (I); The ratio of total CD45.2 and CD45.1 cNK cells in the same chimeras was calculated (J); The ratio of CD45.2 and CD45.1 CD11b^{-}CD27^{+}, CD11b^{+}CD27^{+} and CD11b^{+}CD27^{-} cells in the same chimeras was calculated (K).

(L) T-bet protein amounts in hepatic cNK cells from *Tbx21*$^{+/+}$ (n=5), *Tbx21*$^{\triangle CNS-3}$ (n=3) and *Tbx21*$^{\triangle CNS-3\triangle CNS-8.5}$ (n=3) mice were measured, and T-bet MFI was calculated. Mean ± SD.

Data are representative of two (A, C-L) independent experiments.

Supplemental Figure 3

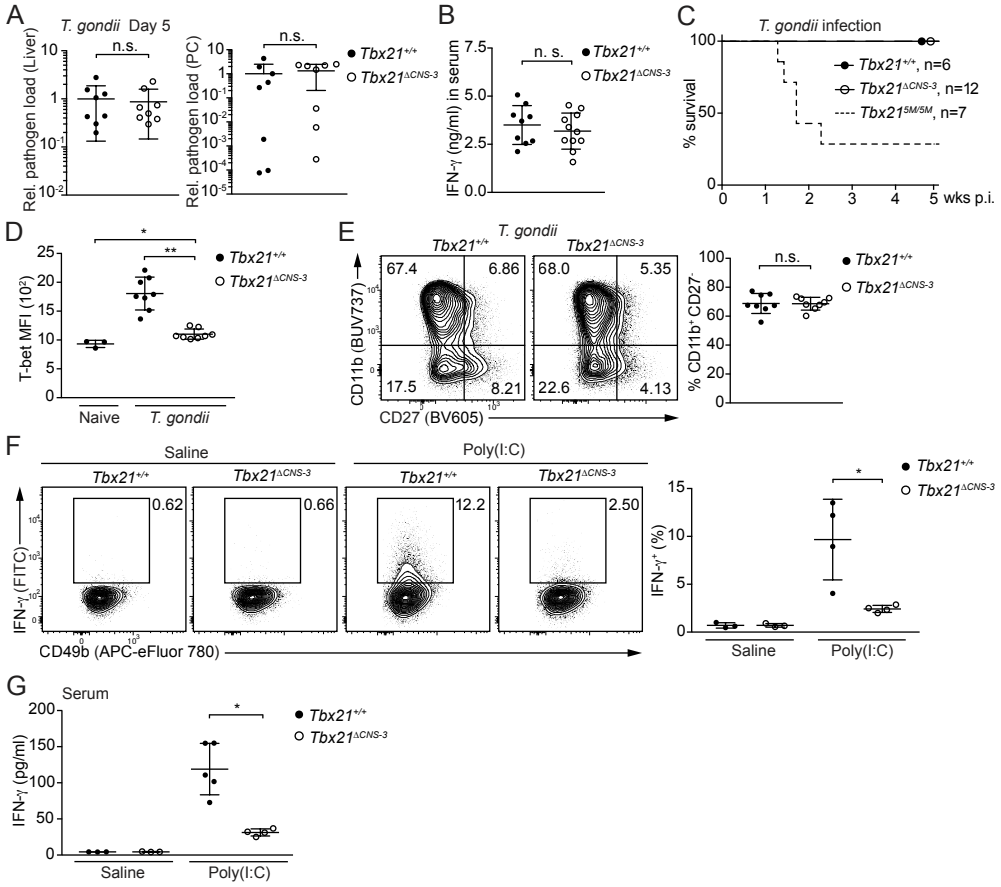

Supplementary Figure 3. The responses of the *Tbx21*$^{\triangle CNS-3}$ mice to *T. gondii* infection and poly (I:C) treatment, related to Figure 2 and Figure 4

(A and B) *Tbx21*$^{+/+}$ (n=8) and *Tbx21*$^{\triangle CNS-3}$ (n=8) mice were infected (*i.p.*) with *T. gondii*. The relative pathogen load in liver and peritoneal cavity (A) and the IFN-γ in the serum (B) were measured after 5 days.

(C) *Tbx21*$^{+/+}$ (n=6), *Tbx21*$^{\triangle CNS-3}$ (n=12) and *Tbx21*$^{5M/5M}$ (n=7) mice were infected with *T. gondii*, and then monitored for their survival.

(D and E) T-bet protein amounts in hepatic cNK cells from naïve *Tbx21*$^{+/+}$ and *T. gondii* infected *Tbx21*$^{+/+}$ and *Tbx21*$^{\triangle CNS-3}$ mice were measured (D). Maturation of cNK cells from infected mice was assessed (E).

(F) *Tbx21*$^{+/+}$ and *Tbx21*$^{\triangle CNS-3}$ mice were treated (*i.p.*) with poly (I:C) or control saline for 2.5 hours, and the hepatic lymphocytes were harvested and incubated with monensin for 3.5 hours before intracellular staining.

(G) *Tbx21*$^{+/+}$ and *Tbx21*$^{\triangle CNS-3}$ mice were treated (*i.p.*) with poly (I:C) or control saline for 6 hours, and the IFN-γ in the serum was measured by ELISA.

Data are representative of two (A-G) independent experiments.

Supplemental Figure 4

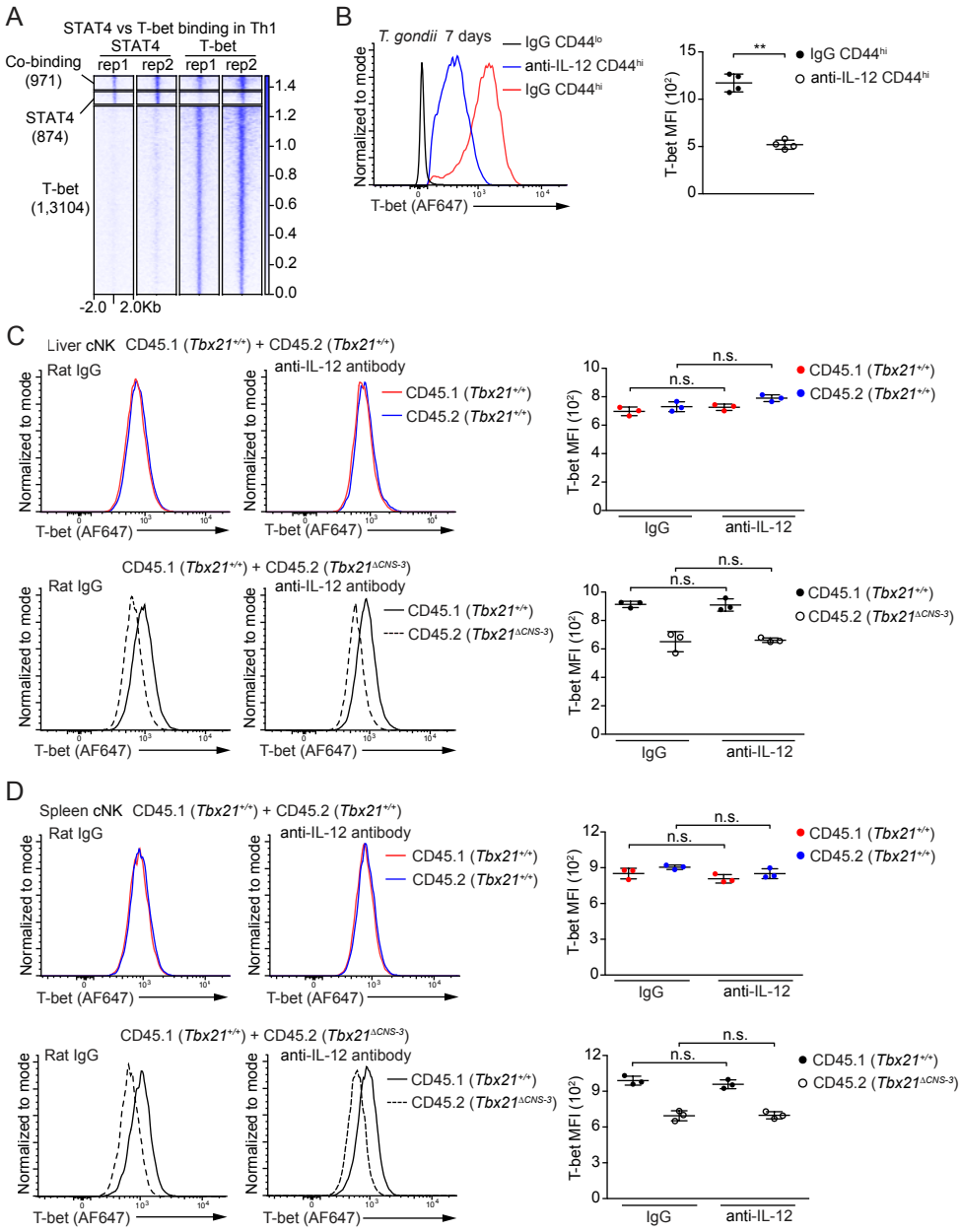

Supplementary Figure 4. STAT4 binding in Th1 cells and the role of IL-12-STAT4 signaling during cNK cell development, related to Figure 3 and Figure 5

(A) STAT4 binding sites and T-bet binding sites in Th1 cells were analyzed. Cell samples are in biological duplicates.

(B) WT mice were pre-treated with control IgG or anti-IL-12 p40 2 days before *T. gondii* infection. After infection, the mice were further treated with these antibodies on day 1 and day 4, and then analyzed on day 7. T-bet protein amounts in $CD4^{+}CD44^{hi}$ and $CD4^{+}CD44^{lo}$ cells were measured, and T-bet MFI was calculated. Mean ± SD, n=4.

(C and D) CD45.1 $Tbx21^{+/+}$ BM cells were co-transferred with either CD45.2 $Tbx21^{+/+}$ or CD45.2 $Tbx21^{\triangle CNS-3}$ BM cells into sub-lethally irradiated $Rag2^{-/-}\gamma c^{-/-}$ recipient mice that were pre-treated with control IgG or anti-IL-12 p40 2 days before to create CD45.1 $Tbx21^{+/+}$/CD45.2 $Tbx21^{+/+}$ (n=3) and CD45.1 $Tbx21^{+/+}$/CD45.2 $Tbx21^{\triangle CNS-3}$ (n=3) mixed chimeras. The chimeras were further treated with control IgG or anti-IL-12 p40 every 5 days starting from day 1. T-bet protein amounts in hepatic cNK cells (C) and splenic cNK cells (D) were measured, and T-bet MFI was calculated 8 weeks after BM transplant. Mean ± SD.

Data are representative of two (B-D) independent experiments.

Supplemental Figure 5

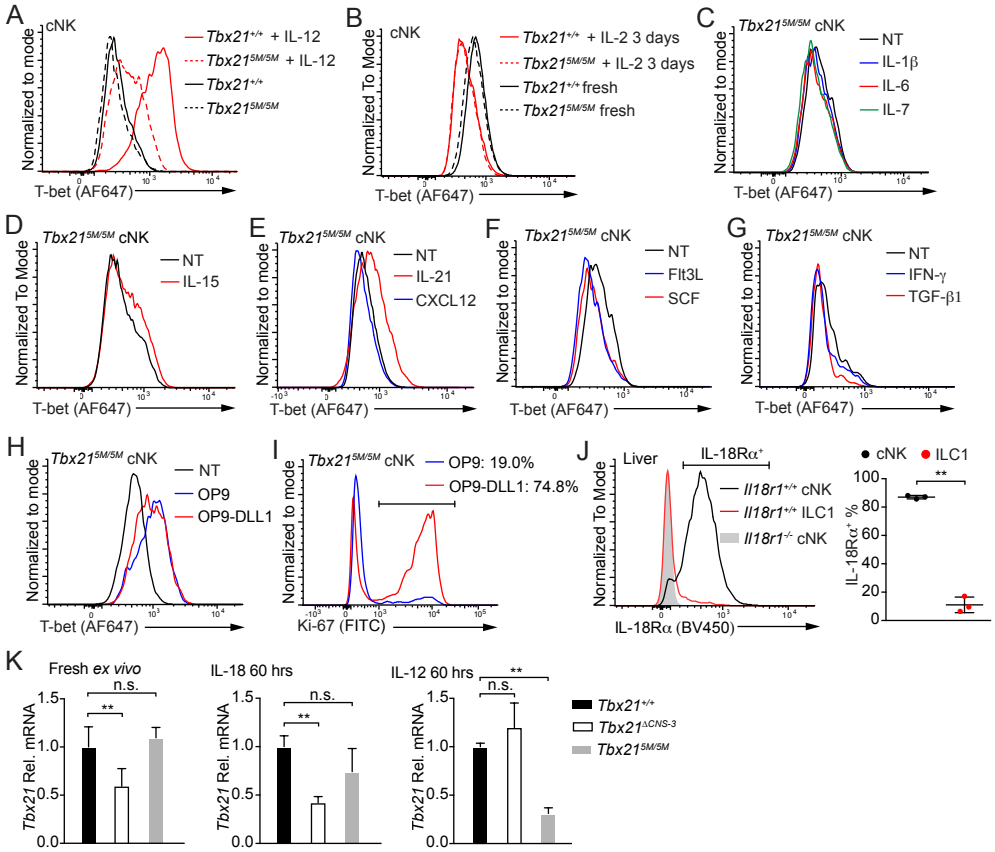

Supplementary Figure 5. Regulation of T-bet expression in cNK cells *in vitro*, related to Figure 5 and Figure 6

(A) T-bet protein amounts in *Tbx21*$^{+/+}$ and *Tbx21*$^{5M/5M}$ cNK cells incubated with or without IL-12 for 3 days in the presence of IL-2 were measured.

(B) T-bet protein amounts in *Tbx21*$^{+/+}$ and *Tbx21*$^{5M/5M}$ cNK cells freshly harvested (black) and cultured 3 days in the presence of IL-2 *in vitro* (red) were measured.

(C-G) T-bet protein amounts in *Tbx21*$^{5M/5M}$ cNK cells incubated with IL-1β, IL-6, IL-7, IL-15, IL-21, CXCL12, Flt3L, SCF, IFN-γ or TGF-β1 for 3 days in the presence of IL-2 were measured.

(H and I) *Tbx21*$^{5M/5M}$ cNK cells were cultured alone (NT) or co-cultured with OP9 or OP9-DLL1 cell line for 3 days in the presence of IL-2. T-bet and Ki-67 protein amounts were measured.

(J) The expression of IL-18Rα on hepatic cNK cells and ILC1s was assessed and the percentage of IL-18Rα^{+} cells was calculated. Mean ± SD, n=3.

(K) T-bet mRNA amounts in *Tbx21*$^{+/+}$ (n=3), *Tbx21*$^{5M/5M}$ (n=3) and *Tbx21*$^{\triangle CNS-3}$ (n=3) splenic cNK cells *ex vivo*, incubated with IL-18 or IL-12 for 60 hours *in vitro* were measured by using qRT-PCR and normalized to *Hprt* mRNA. Mean ± SD.

Data are representative of two (A-K) independent experiments.

Supplemental Figure 6

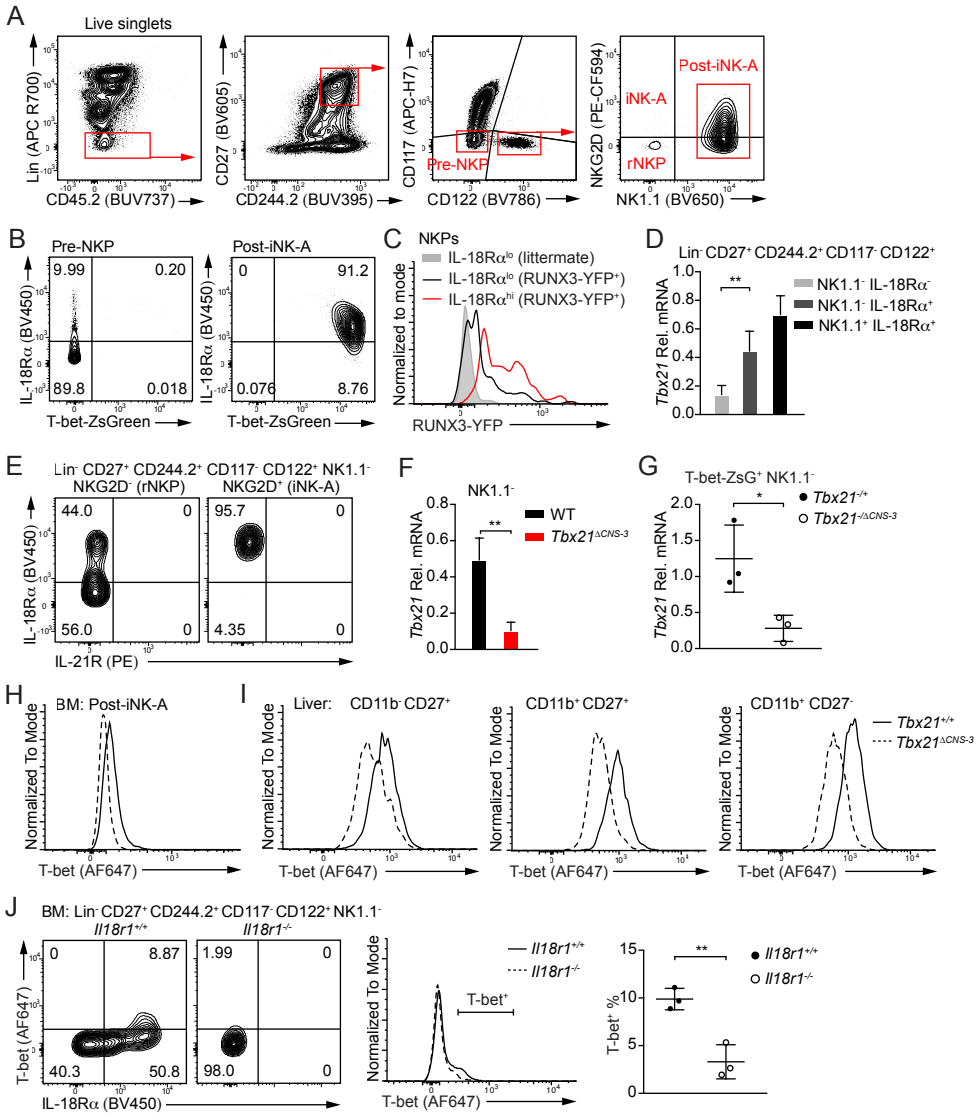

Supplementary Figure 6. IL-18Rα expression is correlated with T-bet expression during NK cell development, related to Figure 6

(A) Gating strategy for detecting pre-NKPs, rNKPs, iNK-A and post-iNK-A cells in BM. The pre-NKPs were gated as Lin$^-$CD27$^+$CD244.2$^+$CD117$^-$CD122$^-$, the rNKPs were gated as Lin$^-$CD27$^+$CD244.2$^+$CD117$^-$CD122$^+$NK1.1$^-$NKG2D$^-$, the iNK-A cells were gated as Lin$^-$CD27$^+$CD244.2$^+$CD117$^-$CD122$^+$NK1.1$^-$NKG2D$^+$, and post-iNK-A cells were gated as Lin$^-$CD27$^+$CD244.2$^+$CD117$^-$CD122$^+$NK1.1$^+$.

(B) The expression of IL-18Rα and T-bet reporter ZsGreen in pre-NKPs and post-iNK-A cells from T-bet-ZsGreen reporter mouse was measured.

(C) The expression of RUNX3-YFP reporter in Lin$^-$CD27$^+$CD244.2$^+$CD117$^-$CD122$^+$NK1.1$^-$IL-18Rα^{lo} and Lin$^-$CD27$^+$CD244.2$^+$CD117$^-$CD122$^+$NK1.1$^-$IL-18Rα^{hi} cells from RUNX3-YFP$^{-/+}$ reporter mice was measured. The Lin$^-$CD27$^+$CD244.2$^+$CD117$^-$CD122$^+$NK1.1$^-$IL-18Rα^{lo} cells from WT littermate were used as negative controls.

(D) The expression of *Tbx21* mRNA in Lin$^-$CD27$^+$CD244.2$^+$CD117$^-$CD122$^+$NK1.1$^-$IL-18Rα$^-$, Lin$^-$CD27$^+$CD244.2$^+$CD117$^-$CD122$^+$NK1.1$^-$IL-18Rα$^+$ and Lin$^-$CD27$^+$CD244.2$^+$CD117$^-$CD122$^+$NK1.1$^+$IL-18Rα$^+$ populations was assessed by using qRT-PCR and normalized to *Hprt* mRNA. Mean ± SD, n=3.

(E) The expression of IL-21R and IL-18Rα in rNKPs and iNK-A cells.

(F) The expression of *Tbx21* mRNA in Lin$^-$CD27$^+$CD244.2$^+$CD117$^-$CD122$^+$NK1.1$^-$ cells from *Tbx21*$^{+/+}$ (n=3) and *Tbx21*$^{\triangle CNS\text{-}3}$ (n=3) mice was assessed by using qRT-PCR and normalized to *Hprt* mRNA. Mean ± SD.

(G) T-bet-ZsGreen-*Tbx21*$^{-/-}$ mice were crossed with *Tbx21*$^{+/+}$ or *Tbx21*$^{\triangle CNS\text{-}3}$ mice to obtain the T-bet-ZsGreen-*Tbx21*$^{-/+}$ (one allele is *Tbx21* KO and the other allele is *Tbx21* WT) and T-bet-ZsGreen-*Tbx21*$^{-/\triangle CNS\text{-}3}$ (one allele is *Tbx21* KO and the other allele is *Tbx21-CNS-3* KO) mice. The expression of *Tbx21* mRNA in Lin$^-$CD27$^+$CD244.2$^+$CD117$^-$CD122$^+$NK1.1$^-$ZsGreen^{hi} cells from T-bet-ZsGreen-*Tbx21*$^{-/+}$ (n=3) and T-bet-ZsGreen-*Tbx21*$^{-/\triangle CNS\text{-}3}$ (n=3) mice was assessed by using qRT-PCR and normalized to *Hprt* mRNA. The assay detected the *Tbx21* transcripts from the WT and *Tbx21-CNS-3 KO* alleles. Mean ± SD.

(H and I) The expression of T-bet in post-iNK-A cells (H), and hepatic CD11b$^-$CD27$^+$, CD11b$^+$CD27$^+$ and CD11b$^+$CD27$^-$ cells (I) from *Tbx21*$^{+/+}$ (n=3) and *Tbx21*$^{\triangle CNS\text{-}3}$ (n=3) mice was measured.

(J) The expression of T-bet in the bulk of rNKPs and iNK-A cells from *Il18r1*$^{+/+}$ (n=3) and *Il18r1*$^{-/-}$ (n=3) BM was measured by intracellular staining. The percentage of T-bet$^+$ cells in the bulk population was calculated. Mean ± SD.

Data are representative of two (B-J) independent experiments.

Supplemental Figure 7

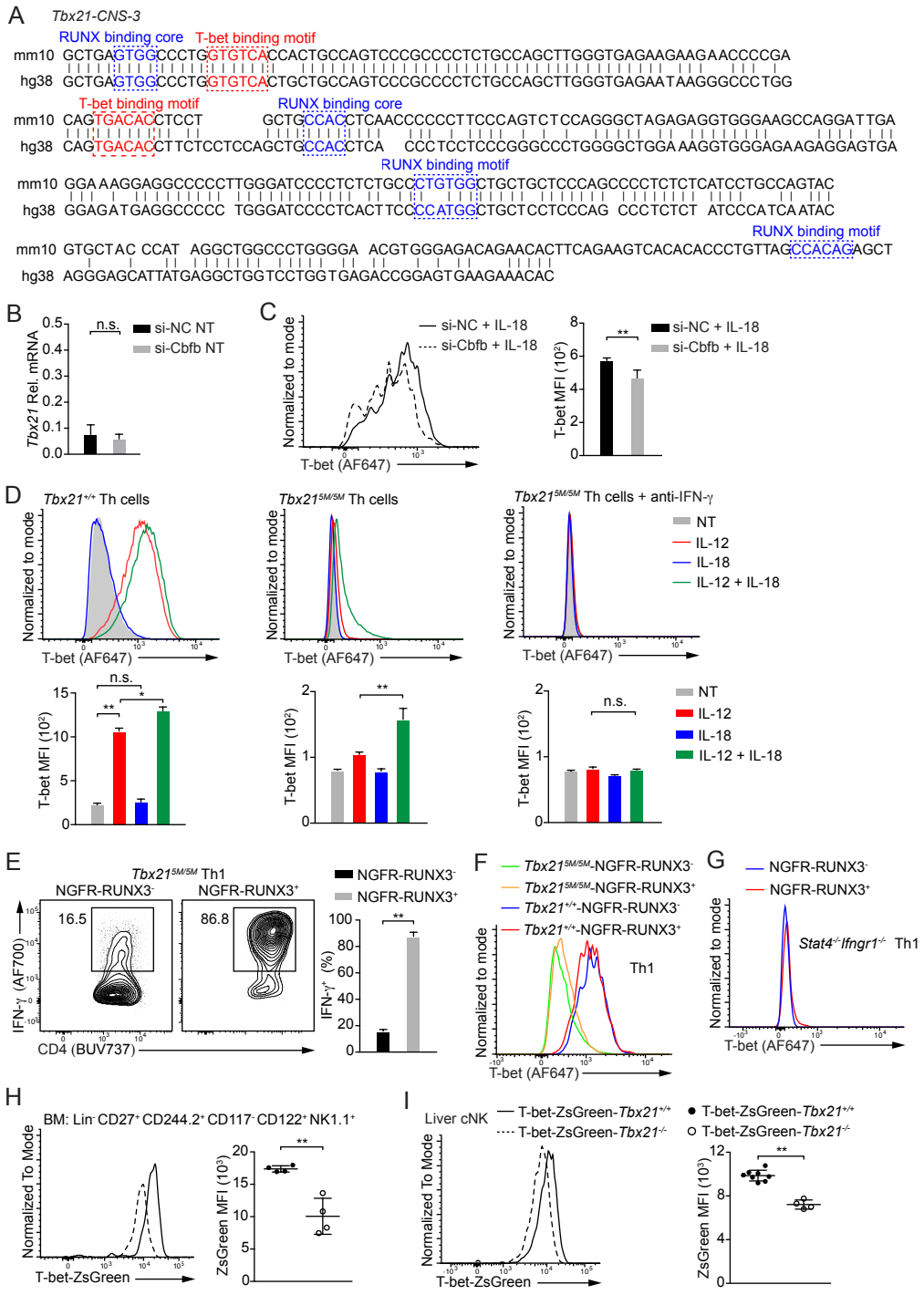

Supplementary Figure 7. Roles of RUNX3 and T-bet for T-bet induction in Th1 and cNK cells, related to Figure 7

(A) T-bet binding motifs (red) and RUNX binding motifs (blue) at *Tbx21-CNS-3* were identified by using the MEME Suite and were highlighted. Two core sequences of RUNX binding (blue) near the T-bet binding motifs were also highlighted. The conservation between human *TBX21-CNS-2.5* and mouse *Tbx21-CNS-3* was shown.

(B) *Tbx21*$^{5M/5M}$ cNK cells were manipulated as Figure 7D without IL-18 incubation. The transcripts of *Tbx21* were assessed by qRT-PCR. Mean ± SD, n=3.

(C) *Tbx21*$^{5M/5M}$ cNK cells were manipulated as Figure 7D except that the cells were incubated with IL-18 for 3 days. T-bet protein amounts were measured, and T-bet MFI was calculated. Mean ± SD, n=3.

(D) Naïve CD4 T cells from the *Tbx21*$^{+/+}$ (n=3) and *Tbx21*$^{5M/5M}$ (n=3) mice were cultured with anti-CD3/CD28, IL-2 and anti-IL-4 in the presence of IL-12 or IL-18 alone or in combination for 3 days and then in the resting conditions for 1 day. T-bet protein amounts were measured, and T-bet MFI was calculated. Mean ± SD.

(E) Naïve CD4 T cells from the *Tbx21*$^{5M/5M}$ mice were cultured under Th1-skewing conditions and infected with NGFR-RUNX3 retrovirus for 4 days. In the presence of monensin, cells were stimulated with PMA and ionomycin for 4 hours. The percentage of IFN-γ-producing cells in NGFR^{-} and NGFR^{+} population was calculated. Mean ± SD, n = 3.

(F and G) Naïve CD4 T cells from *Tbx21*$^{+/+}$ and *Tbx21*$^{5M/5M}$ (F) or *Stat4*$^{-/-}$*Ifngr1*$^{-/-}$ mice (G) were cultured under Th1-skewing conditions and infected with NGFR-RUNX3 retrovirus for 4 days. T-bet protein amounts were measured.

(H) The expression of T-bet-ZsGreen reporter in post-iNK-A cells from T-bet-ZsGreen-*Tbx21*$^{+/+}$ (n=4) and T-bet-ZsGreen-*Tbx21*$^{-/-}$ (n=4) mice was measured, and ZsGreen MFI was calculated. Mean ± SD.

(I) The expression of T-bet-ZsGreen reporter in hepatic cNK cells from T-bet-ZsGreen-*Tbx21*$^{+/+}$ (n=8) and T-bet-ZsGreen-*Tbx21*$^{-/-}$ (n=4) mice was measured, and ZsGreen MFI was calculated. Mean ± SD.

Data are representative of two (B-I) independent experiments.